Synthesis and Crystal Structure of a New Quaternary Chalcoantimonide: $KLa_2Sb_3S_9$ and $KSm_2Sb_3Se_8$

Sung-Jin Kim,* Sunju Park, and Sunah Yim

Department of Chemistry, Ewha Womans University, Seoul 120-750, Korea
Received July 11, 2003

Silver-needle shaped crystals of $KLa_2Sb_3S_9$ from K_2S_x flux and $KSm_2Sb_3Se_8$ from NaCl/KCl flux reactions were obtained and their crystal structures were determined by the single crystal X-ray diffraction method. $KLa_2Sb_3S_9$ crystallizes in the orthorhombic noncentrosymmetric space group $P2_12_12_1$ (No.19) with a unit cell of a = 4.220(3) Å, b = 24.145(2) Å, c = 14.757(5) Å and Z = 4. $KSm_2Sb_3Se_8$ crystallizes in the orthorhombic space group Pnma (No.62) with a unit cell of a = 16.719(3) Å, b = 4.1236(8) Å, c = 22.151(4) Å and Z = 4. Both structures have three-dimensional tunnel frameworks filled with K^+ ions. $KSm_2Sb_3Se_8$ is an ordered version of $ALn_{1-x}Bi_{4\pm x}S_8$, and it is made up of NaCl-type and Gd_2S_3-type fragments. $KLa_2Sb_3S_9$ also contains building fragments similar to those of $KSm_2Sb_3Se_8$, however, there are chalcogen-chalcogen bonds in the Gd_2S_3-type fragment. The formula of $KLa_2Sb_3S_9$ can be described as $(K^-)(La^{3+})_2(Sb^{3-})_3(S^{2-})_5(S_2^{2-})$.

Key Words : Quaternary chalcoantimonide, Rare-earth quaternary, Flux Gd_2S_3-type, Chalcogen-chalcogen bond

Introduction

Many ternary chalcoantimonides of alkaline or alkaline earth, main group metals and transition metals with various structures have been synthesized.[1-3] Rich structural variations in these compounds are derived from the stereochemically active Sb lone pair electrons.[4] Along with the coordinate character of Sb, it is expected that the addition of large electropositive cations such as lanthanides into $[Sb_xQ_y]^{n-}$ building blocks leads to new compounds with a more complex structure. Especially, rare-earth elements may cause unique metal-chalcogen bonding characters due to their large size and high coordination numbers. This strategy also has been applied to synthesize novel multinary chalcoantimonides and some of ternary rare-earth antimony chalcogenides have been reported.[5]

Compared to the diversity of the ternary Bi and Sb chalcoantimonide compounds, rare-earth quaternary phases in this class are quite limited. Reported rare-earth chalcoantimonides are $K_2(RE)_{2-x}Sb_{4+x}Se_{12}$ (RE=La, Ce, Pr, Gd),[6] AU_2SbQ_8 (A=K, Rb; Q=S, Se),[7] $KThSb_2Se_6$,[8] $K_2Gd_2Sb_2Se_9$, $K_2La_2Sb_2S_9$,[9] and $Na_9Gd_5Sb_8S_{26}$,[10] and Bi compounds are $BaLaBi_2S_6$,[8] $Eu_2Pb_2Bi_6Se_{13}$,[11] and $ALn_{1-x}Bi_{4\pm x}S_8$ (A=K, Rb; Ln=La, Ce, Pr, Nd).[12] Here we report on the synthesis and structure of the new quaternary rare-earth chalcoantimonides, $KLa_2Sb_3S_9$ and $KSm_2Sb_3Se_8$.

Experimental Section

Synthesis. $KLa_2Sb_3S_9$ was prepared from the mixtures of ~0.127 g of K_2S_x, 1.13 mmol of La chips (99.9% Aldrich), 4.54 mmol of Sb powder (99.999% Kojundo) and 11.35 mmol of S powder (99.998% Aldrich). K_2S_x was synthesized by a reaction of K metal (99.9% Farco Chemical) and S powder in liquid NH_3. The reacting mixture was loaded in a quartz tube and then doubly sealed in a high vacuum. The mixture was heated slowly up to 700 °C, kept for 10 days, and cooled to room temperature by lowering it at a rate of 2 °C/hr. Silver-needle shaped $KLa_2Sb_3S_9$ crystals were obtained after washing the product with DMF, ethanol and distilled water to remove an excess flux, and were then dried in an oven.

$KSm_2Sb_3Se_8$ was prepared from a mixture of 0.55 mmol Sm chips (99.9% Aldrich), 1.09 mmol of Sb_2Se_3 powder, 1.20 mmol of Se shots (99.99% Aldrich) with ~1.5 g of a 1 : 1 mixture of NaCl/KCl flux. Sb_2Se_3 was directly synthesized by heating a stoichiometric mixture of Sb powder (99.999%, Kojundo) and Se shots. The reacting mixture was loaded in a quartz tube and then doubly sealed in a high vacuum. The mixture was slowly heated up to 750 °C, kept for 10 days, and then cooled to room temperature by lowering it at a rate of 2 °C/hr. Silver needle crystals were obtained by washing the product with distilled water to remove an excess flux, and were then dried in an oven.

The existence of four elements was confirmed qualitatively by an energy-dispersive X-ray (EDX) spectrometer equipped with an electron probe microanalysis (EPMA; JXA-9600, EDX: LinkeXL). Once the stoichiometries were determined, $KLa_2Sb_3S_9$ was prepared rationally as a single phase starting from the exact stoichiometry ratio of the elements and the excess flux of K_2S_x in an evacuated quartz tube. $KSm_2Sb_3Se_8$ was prepared from NaCl/KCl flux with some unknown minor phases. However, almost the single phase of $KSm_2Sb_3Se_8$ was nearly obtained when K_2Se flux was used.

X-ray Crystallography. Silver-needle shaped $KLa_2Sb_3S_9$ crystals were obtained and their crystal structure was determined by the single crystal X-ray diffraction method. A preliminary examination and data collection were performed with Mo $K\alpha_1$ radiation (λ = 0.71073 Å) on an Enraf Nonius diffractormeter (CAD4) equipped with an incident beam

monochromatic graphite crystal. The unit cell parameters and orientation matrix for data collection were obtained from the least-square refinement, using the setting angles of 25 reflections in the range of $18° < 2\theta$ (MoK) $< 25°$. The observed Laue symmetry and systematic extinction suggested the noncentrosymmetric space group $P2_12_12_1$ for $KLa_2Sb_3S_9$. The thermal parameters of S(8) and S(9) were high (0.070 Å^2) compared to the other sulfur atoms. Significant electron densities at distances of 0.64(1) Å and 0.64(1) Å from S(8) and S(9) were found, respectively, and the two electron density peaks were assigned as S(10) and S(11). When the sum of the occupancies of S(8) and S(10) were constrained equal to 100%, their partial occupancies converged to 51% and 49%, respectively, and the occupancies of both S(9) and S(11) converged to 50% under the 100% constraint for the sum. Since we did not observe enough extra reflections from several larger crystals having a much longer exposure period, we exclude the possibility of a superstructure due to an ordering of S atoms.

The final cycle of refinement performed on F_0^2 with 2609 unique reflections converged to the residuals wR_2 ($F_0^2 > 0$) = 0.1434 and conventional R index based on the reflections having $F_0^2 > 2\sigma(F_0^2)$ 0.0515. The complete data collection parameters and details of structure solution and refinement results are given in Table 1. The final atomic positions, displacement parameters, and isotropic displacement parameters are shown in Table 2. Selected bond distances and angles are listed in Table 3.

Silver-needle shaped $KSm_2Sb_3Se_8$ crystals were obtained from the reaction product in NaCl/KCl flux and its crystal structure was determined by the single crystal X-ray diffraction method. The observed Laue symmetry and systematic extinction suggested the space groups $Pna2_1$ and $Pnma$. Subsequent refinements confirmed the centrosymmetric space group $Pnma$. The final cycle of refinement performed on F_0^2 with 1539 unique reflections converged to residuals wR_2 ($F_0^2 > 0$) = 0.1394 and a conventional R index based on the reflections having $F_0^2 > 2\sigma(F_0^2)$ 0.0616. The complete data collection parameters, structure solution details and refinement results are given in Table 1. The final atomic positions, displacement parameters, and isotropic displacement parameters are given in Table 4. Selected bond distances and angles are listed in Table 5.

Table 1. Crystallographic Data of $KLa_2Sb_3S_9$ and $KSm_2Sb_3Se_8$

Empirical formula	$KLa_2Sb_3S_9$	$KSm_2Sb_3Se_8$
Formula weight	970.71	1336.73
Temperature (K)	293(2)	293(2)
Wavelength (λ = Kα, Å)	0.71073	0.71073
Crystal system	Orthorhombic	Orthorhombic
Space group	$P2_12_12_1$ (No.19)	$Pnma$ (No.62)
Unit cell dimensions (Å)	a = 4.220(3)	a = 16.719(3)
	b = 24.145(2)	b = 4.1236(8)
	c = 14.757(5)	c = 22.151(4)
Volume (Å^3)	1503.6(13)	1527.1(5)
Z	4	4
Calculated density (g/cm^3)	4.288	5.814
Absorption coefficient (mm^{-1})	12.370	32.110
θ range for data collection (deg)	2.18 to 24.98	1.53 to 24.97
Reflection collected/unique	3196 / 2609	3173 / 1539
	(R_{int} = 0.0250)	(R_{int} = 0.0483)
Goodness of fit on F^2	1.037	1.158
Data/Restraints/Parameters	2609 / 0 / 152	1539 / 0 / 87
Final R indices [$F_0^2 > 2\sigma(F_0^2)$][a]	R1 = 0.0515	R1 = 0.0616
	wR_2 = 0.1319	wR_2 = 0.1159
R indices ($F_0^2 > 0$)	R1 = 0.0645	R1 = 0.1029
	wR_2 = 0.1434	wR_2 = 0.1394
Largest diff. peak and hole (e Å^{-3})	3.211 and -1.920	4.433 and -5.155

[a] $R1 = [\Sigma \mid |F_o| - |F_c| \mid]/\Sigma |F_o|$. $wR_2 = \{[\Sigma w(|F_o| - |F_c|)^2]/[\Sigma w(F_o^2)^2]\}^{1/2}$; $w = \sigma_F^{-2}$

Table 2. Atomic Coordinates ($\times 10^4$), Occupancy and Equivalent Isotropic Displacement Parameters (Å$^2 \times 10^3$) for $KLa_2Sb_3S_9$

Atoms	x	y	z	Occupancy (%)	U (eq)
La(1)	781(3)	2276(1)	3361(1)	100	13(1)
La(2)	235(3)	9001(1)	928(1)	100	15(1)
Sb(1)	5415(4)	1864(1)	957(1)	100	27(1)
Sb(2)	9817(3)	9668(1)	4965(1)	100	19(1)
Sb(3)	4370(4)	8477(1)	3343(1)	100	21(1)
S(1)	5253(13)	9799(2)	1398(3)	100	16(1)
S(2)	5562(13)	1579(2)	2536(3)	100	17(1)
S(3)	9377(13)	1328(2)	4560(3)	100	16(1)
S(4)	5474(12)	3170(2)	3257(3)	100	14(1)
S(5)	9765(18)	9117(2)	2964(3)	100	31(1)
S(6)	6417(12)	2029(2)	4822(3)	100	16(1)
S(7)	670(2)	9761(2)	9363(4)	100	39(2)
S(8)	9690(7)	2645(5)	1376(7)	51	20(6)
S(10)	1180(8)	2612(5)	1388(7)	49	14(5)
S(9)	1400(2)	1116(13)	506(11)	50	19(9)
S(11)	0(2)	1172(8)	538(10)	50	22(9)
K(1)	153(13)	521(2)	2589(3)	100	28(1)

U(eq) is defined as one-third of the trace of the orthogonalized U_{ij} tensor.

Results and Discussion

$KLa_2Sb_3S_9$. $KLa_2Sb_3S_9$ has a three-dimensional tunnel framework with dumbbell-shaped channels, and K^+ ions are stabilized at the two ends of the channels. The channels run parallel to the a-axis and are linked to each other by La^{3-}-centered infinite rods with a shield-shaped cross-section, as shown Figure 1. The coordination geometry of La(1) is a tricapped trigonal prism with the La(1)-S distances in the range of 2.895(5)-3.265(5) Å. One of the capping sulfur atoms, S(3), forms a S-S dimer with one of prismatic sulfur atoms, S(6), at a distance of 2.139(7) Å; this is in the range of typical dimeric S-S bond distance, a range of 2.096(5)-2.14(1) Å[7,8,9] (Fig. 2(a)). La(2) has a coordinative environment similar to that of La(1), where the La(2)-S distance is in the range of 2.915(5)-3.358(5) Å (Fig. 2(b)). The same S(3)-S(6) dimer is shared by La(1) and La(2)-centered polyhedra; hence, the formula of the compound could be

Table 3. Selected Bond Distances (Å) and Angles (°) for $KLa_2Sb_3S_9$

La(1)-S(2)	2.895(5), 3.027(5)	La(1)-S(6)	2.897(5), 3.176(5) 3.265(5)
La(1)-S(4)	2.933(5), 3.114(5)	La(1)-S(3)	2.953(5)
La(1)-S(10)	3.027(11)	La(1)-S(8)	3.096(13)
La(2)-S(3)	2.915(5), 3.142(5)	La(2)-S(1)	2.934(5), 2.945(5)
La(2)-S(7)	2.956(6)	La(2)-S(4)	2.958(5), 3.358(5)
La(2)-S(5)	3.023(5)	La(2)-S(6)	3.055(5)
Sb(1)-S(2)	2.430(5)	Sb(1)-S(9)	2.56(4), 3.176(70)
Sb(1)-S(11)	2.61(7), 2.91(7)	Sb(1)-S(10)	2.62(3), 3.096(28)
Sb(1)-S(8)	2.682(19), 3.216(24), 3.655(11)	Sb(2)-S(1)	2.477(5)
Sb(2)-S(7)	2.513(7), 2.838(8)	Sb(2)-S(9)	2.59(7), 3.332(69)
Sb(2)-S(11)	2.993(59), 3.100(61)	Sb(2)-S(5)	3.238(5)
Sb(3)-S(4)	2.476(5)	Sb(3)-S(5)	2.544(7), 2.807(7)
Sb(3)-S(8)	2.67(3), 3.239(24)	Sb(3)-S(10)	2.84(2), 3.163(26)
Sb(3)-S(9)	3.356(20)		
S(3)-S(6)	2.139(7)		
K(1)-S(2)	3.207(7), 3.427(7)	K(1)-S(1)	3.227(7), 3.281(7)
K(1)-S(7)	3.229(9), 3.655(9)	K(1)-S(9)	3.435(18)
K(1)-S(5)	3.440(7)	K(1)-S(3)	3.515(7)
S(2)-Sb(1)-S(9)	93.8(4)	S(2)-Sb(1)-S(8)	87.8(3), 178.81(20)
S(2)-Sb(1)-S(11)	91.6(3)	S(2)-Sb(1)-S(10)	88.8(3)
S(9)-Sb(1)-S(8)	178.1(11)	S(10)-Sb(1)-S(11)	175.9(13)
S(1)-Sb(2)-S(9)	97.1(4)	S(7)-Sb(2)-S(9)	92.7(11)
S(7)-Sb(2)-S(7)	104.0(2)	S(1)-Sb(2)-S(5)	175.95(31)
S(4)-Sb(3)-S(5)	89.57(16), 87.32(16)	S(5)-Sb(3)-S(5)	104.00(18)
S(8)-Sb(3)-S(5)	164.6(5)	S(4)-Sb(3)-S(9)	164.6(5)

Table 4. Atomic Coordinates ($\times 10^4$), Occupancy and Equivalent Isotropic Displacement Parameters ($Å^2 \times 10^3$) for $KSm_2Sb_3Se_8$

Atoms	x	y	z	Occupancy (%)	U (eq)
Sm(1)	5356(1)	2500	5896(1)	100	18(1)
Sm(2)	7095(1)	7500	4549(1)	100	19(1)
Sb(1)	8556(1)	2500	6007(1)	100	22(1)
Sb(2)	4643(1)	7500	7393(1)	100	24(1)
Sb(3)	9255(2)	2500	4111(1)	100	39(1)
Se(1)	5951(2)	7500	6686(1)	100	14(1)
Se(2)	7134(2)	2500	5524(1)	100	14(1)
Se(3)	8195(2)	7500	6759(1)	100	19(1)
Se(4)	5323(2)	2500	8239(1)	100	22(1)
Se(5)	8848(2)	7500	4979(1)	100	20(1)
Se(6)	5740(2)	2500	4576(1)	100	15(1)
Se(7)	3941(2)	2500	6743(1)	100	16(1)
Se(8)	7793(2)	2500	3745(1)	100	14(1)
K(1)	7948(5)	7500	2558(3)	100	30(2)

U(eq) is defined as one third of the trace of the orthogonalized U_{ij} tensor.

described as $(K^-)(La^{3-})_2(Sb^{3-})_3(S^{2-})_7(S_2^{2-})$. The coordination environments of La are much like the ones found in the binary LnQ_2(Q=S, Se),[13] where the rare-earth metal atom is coordinated to nine chalcogen atoms in a distorted tricapped trigonal prism. The four La-centered shield- shaped rod comprises two La-centered double columns formed by sharing the S(4)-S(4) edge of two trigonal prisms. Moreover, the two double columns are further condensed in parallel fashion to form a quadruple column in which apex sulfur at S(3) in one double column becomes a cap at S(6) in the next double column (Fig. 2(c)). Comparable infinite polyhedron chains are observed in $KThSb_2Se_6$[8] and $K_2(RE)_{2-x}Sb_{4-x}Se_{12}$ (RE=La, Ce, Pr, Gd).[6] In $KThSb_2Se_6$, Th atoms form one-dimensional infinite double columns that run parallel to the (100) direction. In $ALn_{1\pm x}Bi_{4-x}S_8$.[3] quadruple columns also appears. but with a difference: the two neighboring columns are stacked in a perpendicular fashion.

Three crystallographically different Sb atoms in $KLa_2Sb_3S_9$ have a formal charge of +3 with five coordinations and form dumbbell-shaped channels. Sb(1) has five Sb-S bonds ranging from 2.430(5)-2.682(19) Å. The Sb(1)-S(8) interaction at 3.655(11) Å across the tunnel is considerably longer than the other five Sb(1)-S bond lengths, but still shorter than the sum of the Sb-S van der Waals radii. 4.05 Å.[1(d)] Therefore, the local geometry around Sb(1) is pseudo-octahedral with one long Sb-S interaction. The basal S-Sb(1)-S angles range from 88.2(7)° to 95.8(19)° and the axial S-Sb(1)-S angle is 175.81(20)°: this is also suitable for distorted octahedral coordination. Sb(2) and Sb(3) atoms have coordinate characters similar to that of the Sb(1) atom with five shorter Sb-S bonds at a distance of 2.477(5)-2.993(59) Å for Sb(2) and 2.476(5)-2.807(7) Å for Sb(3). The longer Sb-S bonds at 3.238(5) Å and 3.356(20) Å also exist around Sb(2) and Sb(3), respectively. The basal bond angles are 90.25(16)-104.0(2)° in $Sb(2)S_5$ and 81.3(3)-104.00(18)° in $Sb(3)S_5$, and

Table 5. Selected Bond Distances (Å) and Angles (°) for $KSm_2Sb_3Se_8$

Sm(1)-Se(1)	2.883(2) × 2	Sm(1)-Se(6)	2.950(2) × 2, 2.993(3)
Sm(1)-Se(7)	3.020(3)	Sm(1)-Se(2)	3.085(3)
Sm(2)-Se(8)	2.964(2) × 2	Sm(2)-Se(2)	2.987(2) × 2
Sm(2)-Se(6)	3.063(3) × 2	Sm(2)-Se(5)	3.082(4)
Sm(2)-Se(7)	3.345(3)		
Sb(1)-Se(2)	2.606(4)	Sb(1)-Se(3)	2.719(3) × 2
Sb(1)-Se(5)	3.110(3) × 2	Sb(1)-Se(4)	3.394(4)
Sb(2)-Se(1)	2.689(4)	Sb(2)-Se(7)	2.774(3) × 2
Sb(2)-Se(4)	3.010(3) × 2	Sb(2)-Se(3)	3.064(4)
Sb(3)-Se(8)	2.575(4)	Sb(3)-Se(5)	2.900(3) × 2, 3.758(4)
Sb(3)-Se(4)	2.913(3) × 2		
K(1)-Se(4)	3.261(9)	K(1)-Se(3)	3.322(6) × 2
K(1)-Se(8)	3.352(6) × 2	K(1)-Se(1)	3.371(6) × 2
K(1)-Se(7)	3.517(8)		
Se(2)-Sb(1)-Se(3)	92.84(10)	Se(3)-Sb(1)-Se(3)	98.65(12)
Se(3)-Sb(1)-Se(5)	88.89(6), 170.49(1)	Se(2)-Sb(1)-Se(4)	174.76(12)
Se(5)-Sb(1)-Se(5)	83.05(0)	Se(7)-Sb(2)-Se(7)	96.00(12)
Se(7)-Sb(2)-Se(4)	172.67(11), 88.49(6)	Se(4)-Sb(2)-Se(4)	86.48(11)
Se(1)-Sb(2)-Se(3)	177.74(13)	Se(7)-Sb(2)-Se(3)	89.08(9)
Se(8)-Sb(3)-Se(5)	89.21(11), 165.96(13)	Se(5)-Sb(3)-Se(5)	90.61(13)
Se(5)-Sb(3)-Se(4)	179.51(13), 89.63(6)	Se(4)-Sb(3)-Se(4)	90.12(12)

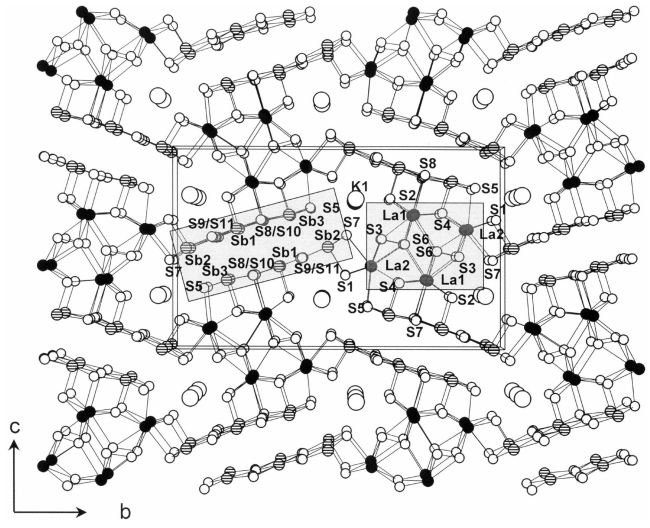

Figure 1. A perspective view of $KLa_2Sb_3S_9$ down the a-axis with the atom labeling. Dumbbell-shaped tunnels, S(3)-S(6) dimers, and the unit cell boundary are shown. The Gd_2S_3-type and NaCl-type building blocks are shaded.

the axial angles are 172.81(14)° for $Sb(2)S_6$ and 175.95(31)° for $Sb(3)S_6$. The distorted environments around Sb atoms indicate that the 5s lone pair electrons in Sb is stereochemically expressed and is directed toward the longer Sb-S bonds.[4] This type of Sb-S coordination is present in Sb_2S_3,[14] $Cs_2Sb_4S_8$[1(d)], and $K_2(RE)_{2-x}Sb_{4+x}Se_{12}$(RE=La, Ce, Pr, Gd).[6]

The potassium atoms observed are coordinated by nine sulfur atoms in a tricapped trigonal prismatic site with an average K-S distance of 3.379(9) Å. $KLa_2Sb_3S_9$ and $KSm_2Sb_3Se_8$ seem to be closely related in their structure and empirical formula. However, they differ in that $KLa_2Sb_3S_9$ contains chalcogen-chalcogen bonds in shield-shape rods; this is not found in KSm_2Sb_3Se.[8] Such a complex feature with S-S bondings in the framework seems to be related to a larger size difference between La and S atoms.

$KSm_2Sb_3Se_8$. $KSm_2Sb_3Se_8$ has a three-dimensional tunnel framework consisting of Gd_2S_3-type and NaCl-type fragments, as shown Figure 3. The shield-shaped Gd_2Se_3-type chain contains two columns of 7-coordinate Sm(1)-centered chain and two columns of 8-coordinate Sm(2)-centered chain. The local geometry of Sm(1) is a distorted monocapped trigonal prism, and the distance between Sm(1) and Se atoms is in the range of 2.883(2)-3.085(3) Å, where Se(7) at 3.020 Å is described as a capping atom (Figure 4(a)). On the other hand, the Sm(2) is located at the center of a distorted bicapped trigonal prism. The distances between Sm(2) and prismatic Se atoms are in the range of 2.964(2)-3.063(3)Å, while the two capping Se(5) and Se(7) atoms are bonded to Sm(2) at distances of 3.083(4) Å and 3.345(3) Å, respectively (Figure 4(b)). The two monocapped prisms stack by sharing their Se(1)-Se(6) edges, while the two bicapped prisms stack by sharing their Se(2)-Se(6)-Se(8) trigonal faces. The two different kinds of prisms are piled and thereby create infinite rods in the (010) direction (see Figure 4(c)). A similar infinite rod was found in Ln_2Q_3 (Ln =Gd, La, Sm; Q=S, Se).[15]

The rectangular-shaped NaCl-type fragments in this compound are made up of three crystallographic different Sb^{3+} atoms. Sb(1)-centered polyhedra have three shorter Sb-Se bonds (2.606(4)-2.719(3) Å) and three longer bonds (3.110(3)-3.394(4) Å); this suggests that the coordination environment of Sb(1) is intermediate between a trigonal bipyramid and an octahedron. However, the longest Sb(1)-Se distance at 3.394(4) Å is shorter than the sum of

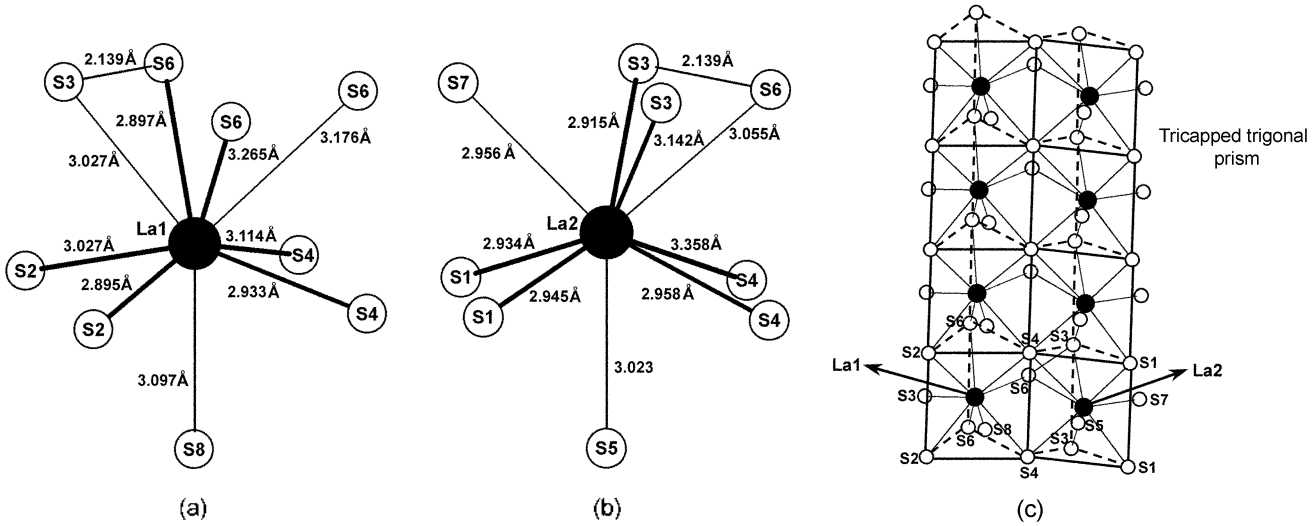

Figure 2. (a) Local coordination of La(1) with the bond distances (Å) in $KLa_2Sb_3S_9$. One of the capping S atoms, S(3) is bonded to a prismatic sulfur atom S(6) at 2.139 Å. S(6) and S(8) are capping sulfur atoms. (b) The local coordination of La(2) with the bond distances (Å). The same S(3)-S(6) dimer is shared by La(1) and La(2)-centered polyhedra. S(6) at 3.055 Å, S(5), and S(7) are capping sulfur atoms. (c) The orientation of two La-centered double columns made of two La(1)S_9 and La(2)S_9 polyhedron.

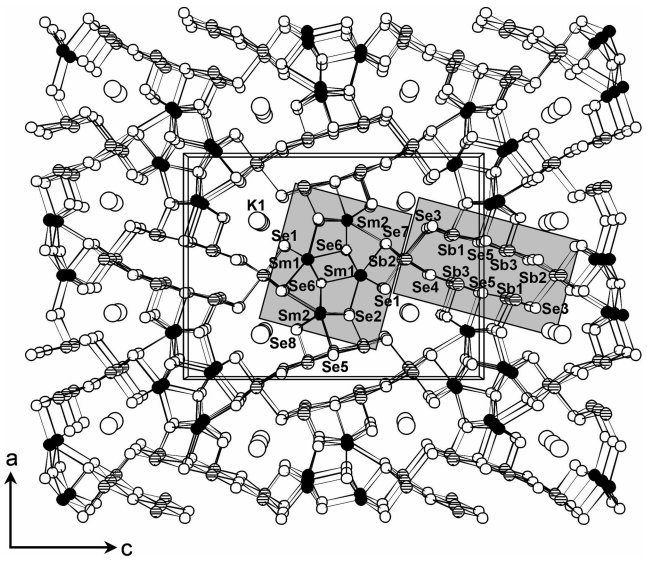

Figure 3. A perspective view of $KSm_2Sb_3Se_8$ down the b-axis with the atom-labeling scheme. The K^+ stabilized tunnels and rectangular shaped tunnels are shown. The unit cell boundary is also shown. The Gd_2S_3-type and NaCl-type building blocks are shaded.

the Sb-Se van der Waals radii, 4.20 Å.[16] Therefore, the local geometry of Sb(1) can be regarded as a pseudo octahedron rather than a trigonal pyramid. The basal Se-Sb(1)-Se angles range from 83.05° to 102.91°, and the axial bond angle is 174.76(12)°, so it is reasonable to regard this as a distorted octahedral coordination. In Sb(2)-centered polyhedra, all Sb-Se bonds are in the normal range, 2.689(4)-3.064(4) Å, with three shorter bonds. The Sb(3)-centered polyhedron seems to form a octahedron with one square plane and two apexes. The Sb(3)-Se bonds in the square plane is 2.900(3) Å and 2.913(3) Å, while the Sb(3)-one apex Se(8) is 2.575(4) Å; Sb(3)-the other apex-Se(5) is 3.758(4) Å, shorter than 4.20 Å. In addition, the bond angles are 89.1(11)-91.22(11)° in the basal plane and the axial bond angle is 163.93°(13) around Sb(3). Thus it is also reasonable that the local geometry of Sb(3) is distorted octahedral, such as in the Sb(1)Se_6 octahedra. That the distorted environments around Sb atoms involved 5s lone pair electrons of Sb was stereochemically expressed and tended toward the longer Sb-Se bonds.[9] The Sb(1)Se_6, Sb(2)Se_6 and Sb(3)Se_6 octahedra were alternatively located by sharing Se atoms in the basal planes to form a rectangular-shaped tunnel running along the b-axis (Figure 3). This kind of fragment is prevalent in M_2Q_3 (M=As, Sb, Bi; Q=S, Se, Te)[17] and also found in $Cs_2Sb_4Se_8$[18] and $K_2(RE)_{2-x}Sb_{4+x}Se_{12}$ (RE=La, Ce, Pr, Gd).[6]

The shield-shaped infinite rods and rectangular-shaped tunnels connect to each other through Sb(2) atoms to build up K^+-filled tunnels. K^+ ions are coordinated with eight Se atoms in the range of 3.261(9)-3.517(8) Å to form distorted bicapped trigonal prisms. $KSm_2Sb_3Se_8$ has structural features similar to those of $ALn_{1-x}Bi_{4-x}S_8$ (A=K, Rb; Ln=La, Ce, Pr, Nd).[12] Gd_2S_3[19] and NaCl-type fragments in $KSm_2Sb_3Se_8$ have the same structural feature as do those in $KLa_{1-x}Bi_{4-x}S_8$. The only difference in the two compounds is the disorders between Ln and Bi atoms; this disorder results in nonstoichiometric composition in $ALn_{1-x}Bi_{4-x}S_8$. However, no partial occupancy and disorder in the Sm and Sb atom sites were detected in $KSm_2Sb_3Se_8$. The ionic radii of La^{3+} and Bi^{3+} are in the ranges of 1.10-1.160 Å and 0.96-1.03 Å, respectively, while those of Sm^{3+} and Sb^{3-} are in the range of 1.02-1.079 Å and 0.76-0.80 Å, respectively.[20] The disorder and mixed occupancy in the Ln and Bi sites in $ALn_{1-x}Bi_{4-x}S_8$ and ordered ideal structure of $KSm_2Sb_3Se_8$ can be understood in terms of the size differences of the two cations, Sm and Sb.

In summary, $KSm_2Sb_3Se_8$ and $KLa_2Sb_3S_9$ commonly consist of Gd_2S_3-type and NaCl-type fragments. $KSm_2Sb_3Se_8$

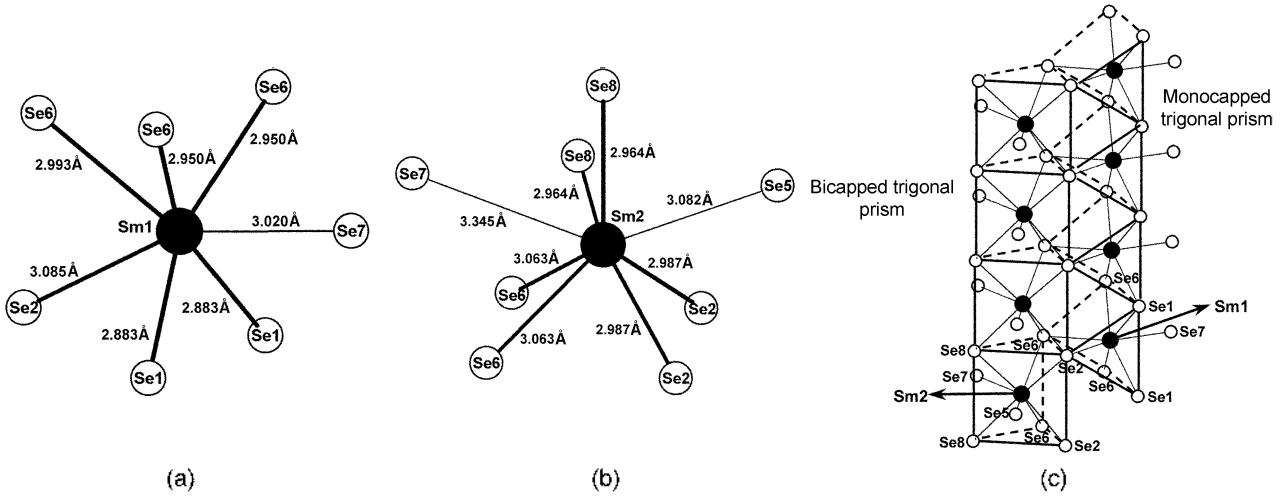

Figure 4. (a) Local coordination of Sm(1) with the bond distances (Å) showing the monocapped trigonal prism. Se (7) is a capping atom. (b) The local coordination of Sm(2) with the bond distances (Å) showing the bicapped trigonal prism. Se(7) and Se(5) are capping atoms. (c) The orientation of the two La-centered double columns consisted of two monocapped and two bicapped trigonal prisms.

phase is an ordered phase of $KLa_{1-x}Bi_{4-x}S_8$, and is due to the larger size differences of the two cations of Sm and Sb. $KLa_2Sb_3S_9$ is a derivative of $KSm_2Sb_3Se_8$ where S-S dimers exist in a Gd_2S_3-type fragment. $KLa_2Sb_3S_9$ demonstrates that the strategy of adding larger rare earth metals to a $(Sb_xQ_y)^{n-}$ building block results in a more complex structure through the fine-tuning of the $(Sb_xQ_y)^{n-}$ building block. Therefore, many more new $(Sb_xQ_y)^{n-}$ building blocks could be prepared using a similar approach.

Acknowledgements. This work is supported from Korea Research Foundation Grant (KRF-2000-015-DP0224).

References

1. (a) Doerrscheidt, W.; Shäfer, H. *Z. Naturforsch.* **1981**, *36B*, 410. (b) Cordier, G.; Schäfer, H. *Rev. Chim. Miner.* **1981**, *18*, 218. (c) Eisenmann, B.; Schäfer, H. *Z. Naturforsch.* **1979**, *34B*, 383. (d) McCarthy, T. J.; Kanatzidis, M. G. *Inorg. Chem.* **1994**, *33*, 1205.
2. (a) Smith, P. P. K.; Hyde, B. G. *Acta Cryst.* **1983**, *C39*, 1498. (b) Skowron, A.; Brown, I. D. *Acta Cryst.* **1990**, *C46*, 527.
3. (a) Lemoine, P. P.; Carré, D.; Robert, F. *Acta Cryst.* **1991**, *C47*, 938. (b) Wacker, K.; Salk, M.; Decker-Schultheiss, G.; Keller, E. *Z. Anorg. Allg. Chem.* **1991**, *606*, 51. (c) Odink, D. A.; Carteaux, V.; Payen, C.; Ouvrard, G. *Chem. Mater.* **1993**, *5*, 237.
4. Olivier-Fourcade, J.; Ibanez, A.; Jumas, J. C.; Maurin, M.; Lefebvre, I.; Lippens, P.; Lannoo, M.; Allan, G. *J. Solid State Chem.* **1990**, *87*, 366.
5. (a) Rustamov, P. G.; Khasaev, J. P.; Aliev, O. M. *Inorg. Mater.* **1981**, *17*, 1469. (b) Aliev, O. M.; Maksudova, T. F.; Samsonova, N. D.; Finkelshtein, L. D.; Rustamov, P. G. *Inorg. Mater.* **1986**, *22*, 23. (c) Alieva, Z. G.; Khasaev, D. P.; Namazov, F. A.; Aliev, F. G.; Aliev, O. M. *Russ. J. Inorg. Chem.* **1988**, *33*, 914.
6. Chen, J. H.; Dorhout, P. H. *J. Alloys and Compds.* **1997**, *249*, 199.
7. Choi, K.-S.; Kanatzidis, M. G. *Chem. Mater.* **1999**, *11*, 2613.
8. Choi, K.-S.; Iordanidis, L.; Chondroudis, K.; Kanatzidis, M. G. *Inorg. Chem.* **1997**, *36*, 3804.
9. Choi, K.-S.; Hanko, J. A.; Kanatzidis, M. G. *J. Solid State Chem.* **1999**, *147*, 309.
10. Park, S.; Kim, S.-J. *J. Solid State Chem.* **2001**, *161*, 129.
11. Chung, D.-Y.; Iordanidis, L.; Choi, K.-S.; Kanatzidis, M. G. *Bull. Korean Chem. Soc.* **1998**, *19*, 1283.
12. Iordanidis, L.; Schindler, J. L.; Kannewurf, C. R.; Kanatzidis, M. G. *J. Solid State Chem.* **1999**, *143*, 151.
13. (a) Chen, J. H.; Dorhout, P. K. *J. Solid State Chem.* **1995**, *117*, 318. (b) Lee, S.; Foran, B. *J. Am. Chem. Soc.* **1994**, *116*, 154.
14. Hoffmann, W. *Z. Z. Kristallogr.* **1933**, *86*, 225.
15. (a) Schleid, T. *Z. Anorg. Allg. Chem.* **1990**, *111*. (b) Grundmeier, T.; Urland, W. *Z. Anorg. Allg. Chem.* **1992**, 1977.
16. Tideswell, N. W.; Kruse, F. H.; McCullough, J. D. *Acta Cryst.* **1957**, *10*, 99.
17. (a) Smith, M. J.; Knight, R. J.; Spencer, C. W. *J. Appl. Phys.* **1962**, *33*, 2186. (b) Testardi, L. R.; Bierly, J. N., Jr.; Donahoe, F. J. *J. Phys. Chem. Solids* **1962**, *23*, 1209. (c) Champness, C. H.; Chiang, T. P.; Parekh, P. *J. Phys.* **1965**, *43*, 653. (d) Yim, W. M.; Fitzke, E. V. *J. Electrochem. Soc.* **1968**, *115*, 556.
18. Sheldrick, W. S.; Kaub, J. *Z. Anorg. Allg. Chem.* **1989**, *536*, 114.
19. Prewitt, C. T.; Sleight, A. W. *Inorg. Chem.* **1968**, *7*, 1090.
20. Shannon, R. D. *Acta Cryst.* **1976**, *A32*, 751.